Journal of Statistical Physics, Vol. 28, No. 4, 1982

Bimodality and Long-Range Order in Ideal Bose Systems

Udayan Mohanty,[1,2] Biman Bagchi,[3,4] and Julian H. Gibbs[3,5]

Received June 23, 1981

The cluster expansion for the classical and the quantum canonical partition function are related to the Bell polynomials. This observation is exploited in derivation of a set of recursion relations that render tractable numerical evaluation of quantities such as mean cluster size distributions and pressure isotherms. The exact volume dependences of properties of an ideal Bose gas are calculated under periodic boundary conditions. Numerical calculations with volume-independent cluster integrals show bimodal distributions in the mean cluster weight for two- and three-dimensional ideal Bose gases at sufficiently low temperature and high density. The variation of the size at which the liquid (condensate) peak appears indicates that the liquid clusters are macroscopic in macroscopic systems. The similarity between the Bose–Einstein condensation and the sol→gel transition in nonlinear chemically polymerizing systems is discussed. When the exact volume dependence of the cluster integrals is taken into account, the mean cluster weight distribution becomes "chair shaped" rather than bimodal and displays no diagonal long-range order in the canonical ensemble. The "Kac density" for an ideal Bose gas implies that in the canonical ensemble the Ursell function satisfies a cluster property in the limit in which the coordinates of the particles are widely separated.

KEY WORDS: Cluster expansion; Bell polynomials; Bose–Einstein condensation; cluster size distribution; Kac density.

1. INTRODUCTION

Bose–Einstein condensation (BEC) in finite systems[1,2] has been the subject of renewed interest, because this "transition" in ideal Bose systems

[1] Department of Physics, Brown University, Providence, Rhode Island 02912.
[2] Present address: Urey Hall, B-014, University of California at San Diego, La Jolla, California 92093.
[3] Department of Chemistry, Brown University, Providence, Rhode Island 02912.
[4] Present address: The James Franck Institute, University of Chicago, Chicago, Illinois 60637.
[5] Present address: Office of the President, Amherst College, Amherst, Massachusetts 01002.

0022-4715/82/0800-0685$03.00/0

(IBS) provides a model, albeit a rather crude one, of the superfluid transition in real helium. In recent years several authors[2] have carried out analytic calculations of the effects of finite size and of surfaces on its critical behavior.

In this paper a new formalism is introduced for calculation of cluster size distributions in IBS: we relate the question of formation of diagonal long range order (DRLO) in IBS to that of bimodality in the ensemble average cluster weight distribution.

For a system of N bosons enclosed in a hypercube of volume L^d, where d is the dimensionality of the system and L is the length of a side of the cube, Kahn and Uhlenbeck have shown that the quantum mechanical partition function $Q_N(T, L^d)$ can be written as a cluster expansion[3] in the form

$$Q_N(T, L^d) = N! \sum_{\substack{\{m_k\} \\ \sum k m_k = N}} \prod_{k=1}^{N} \frac{\left[(L/\lambda)^d b_k\right]^{m_k}}{m_k!} \tag{1.1}$$

analogous to the well-known Mayer formula for classical particles. The $b_k(T, L^d)$'s are the kth connected cluster integrals, in which the symmetry properties of otherwise *noninteracting* bosons play a mathematical role equivalent to that of a potential energy of interaction in the case of *interacting* particles in a classical gas. λ is the thermal wavelength and the m_k's are integers that are positive or zero. Thus, the evaluation of thermodynamic properties for any system involves two nontrivial steps: calculations of the connected cluster integrals and evaluation of the partition function through Eq. (1.1).

In Section 2, the partition function of Eq. (1.1) for a system of N particles $Q_N(T, L^d)$ is shown to be related to the Nth Bell polynomial.[4,5] Exploiting the properties of the Bell polynomials, we find a recursion relation among them and apply it to $Q_{N+1}(T, L^d)$. In Section 2.2, appropriate generating functions are defined that enable derivation of simple recursive formulas for the cluster size distribution and such thermodynamic quantities as pressure isotherms.

It should be emphasized that the methodology in Section 2 is general and can be applied to a wide class of many-body systems. The main requirement is that some information be available about the behavior of either the connected cluster integrals or the star (doubly connected) integrals. We have, for example, been able to study the cluster size distribution for classical systems[6,7] interacting via the Lennard–Jones or the square-well potential. For such classical systems, the first five star integrals[8] are known. Details of such calculations are beyond the scope of this paper and are to be discussed elsewhere.[6,7]

In Section 3.1 we treat in two- and three-dimensions the hypothetical case of IBS in which the volume-dependent cluster integrals $b_k(T, V)$ are replaced by their well-known values, $b_k(T, \infty) \equiv b_k(T)$, in the infinite-volume limit. Although the problem of evaluating the more realistic volume-dependent $b_k(T, V)$ and using them in the calculations of thermodynamic properties is tractable and treated in Section 3.3, the hypothetical case involving the $b_k(T, \infty)$ is devoid of interest in that it has been treated by other methods, the results of which can provide a check on the methods of this paper. Results are obtained in Section 3.1 for the cluster size distribution, $\overline{m}_k(T, V, N)$, in this hypothetical case, results which signal the explosive growth of clusters to macroscopic size. In a graph with $k\overline{m}_k$ as ordinate and k as abscissa, a vertical scaling of the gas peak as contrasted with a horizontal scaling of the "liquid" (condensate) peak with varying system size N clearly shows that in macroscopic systems, the liquid clusters are macroscopic. These results of Section 3.1 throw some new light onto the similarity[5,9,10] between the BEC of an ideal Bose gas and the equilibrium sol $\rightarrow$ gel transition. This is discussed in Section 3.2.

In Section 3.3, a technique is outlined that enables calculation of the exact volume dependence of the connected cluster integrals of IBS enclosed in a hypercube of volume L^d, only periodic boundary conditions being discussed in this paper. The main emphasis in this section is on study of the effect of volume dependence of $b_k(T, V)$ on the cluster size distribution, i.e., on the existence or nonexistence of DLRO of IBS in the canonical ensemble. Numerical calculations with the exact set of $b_k(T, V)$ give results for the distribution $k\overline{m}_k(T, V, N)$ that are significantly different from those obtained for the more artificial case treated in Section 3.1. The results obtained for this more realistic case in Section 3.3 are discussed in detail in Appendix B, in terms of the cluster property of the Ursell functions. Our conclusions are summarized in Section 3.4.

2. RECURSION FORMULAS

2.1. Partition Function and Bell Polynomials

The Bell polynomials[4] studied extensively by E. T. Bell arise in an effort to simplify the taking of the nth derivative, $H_n(x)$, of a composite function,

$$H(x) = F(g(x)) \tag{2.1}$$

It is clear that

$$\begin{aligned} H_1 &= F_1(g(x))g_1(x) \equiv F_1 g_1 \\ H_2 &= F_1 g_2 + G_2 g_1^2 \end{aligned} \tag{2.2}$$

By mathematical induction, it follows that

$$H_n = F_1 A_{n1}(g_1, \ldots, g_n) + \cdots + F_n A_{nn}(g_1, \ldots, g_n) \tag{2.3}$$

$A_{nj}(g_1, \ldots, g_n)$ is a homogeneous polynomial of degree j in $g_1, \ldots, g_n$. Thus, the study of H_n can be reduced to study the structure of Bell polynomials

$$Y_n(g_1, \ldots, g_n) = \sum_{j=1}^{n} A_{nj}(g_1, \ldots, g_n) \tag{2.4}$$

Let $F(g(x)) = e^{g(x)}$ in (2.1); this gives the simple formula

$$Y_n(g_1, \ldots, g_n) = e^{-g(x)} \frac{d^n}{dx^n} e^{-g(x)} \equiv e^{-g} D_x^n e^g \tag{2.5}$$

From this formula, a recurrence relation for the Bell polynomials can be derived:

$$Y_{n+1}(g_1, g_2, \ldots, g_{n+1}) = e^{-g} D_x^{n+1} e^g \tag{2.6}$$

$$= \sum_{k=0}^{n} \binom{n}{k} \left[e^{-g} D_x^{n-k} e^g \right] D_x^k g_1 \tag{2.7}$$

$$= \sum_{k=0}^{n} \binom{n}{k} Y_{n-k}(g_1, \ldots, g_{n-k}) g_{k+1} \tag{2.8}$$

This is the crucial equation exploited in this work.

An explicit form for $Y_n(g_1, \ldots, g_n)$ remains to be found. The generating function of the Bell polynomials is defined as

$$B(t) = \sum_{n=0}^{\infty} \frac{Y_n t^n}{n!} \tag{2.9}$$

Then

$$\ln B(t) = \sum_{n=1}^{\infty} g_n \frac{t^n}{n!} \tag{2.10}$$

To get an explicit representation formula for the Bell polynomials, (2.10) is exponentiated:

$$B(t) = \sum_{n=0}^{\infty} \frac{Y_n t^n}{n!} = \sum_{n=0}^{\infty} t^n \sum_{\substack{\{m_k\} \\ \sum k m_k = n}} \prod_{k=1}^{n} \frac{g_k^{m_k}}{(k!)^{m_k} m_k!} \tag{2.11}$$

Comparing the coefficient of t^n on two sides yields

$$Y_n = n! \sum_{\substack{\{m_k\} \\ \sum k m_k = n}} \prod_{k=1}^{n} \left(\frac{g_k}{k!} \right)^{m_k} \frac{1}{m_k!} \tag{2.12}$$

From equations (2.12) and (1.1), it is noted that the partition function for a system of N particles enclosed in a volume V at temperature T is related[5] to the Nth Bell polynomial:

$$Q_N(T,V) = Y_N\left(1!\frac{Vb_1}{\lambda^d}, 2!\frac{Vb_2}{\lambda^d}, \ldots j!\frac{Vb_j}{\lambda^d}, \ldots, N!\frac{Vb_N}{\lambda^d}\right) \quad (2.13)$$

where b_j is the jth connected integral.

The mathematical structure of the partition function for volume-independent $b_j(T)$ can be shown to lie in the Umbral algebra.[11] Further, this algebra can be used for rederivation[12] of Mayer's "first theorem"[13] and the recursion relation for Bell polynomials.

2.2. Cluster Size Distribution and Pressure

As long as the b_k's are positive definite, an average number of mathematical clusters $\bar{m}_k(T,V,N)$ of size k can be defined as

$$\bar{m}_k(T,V,N) = \left[\sum_{\{m_j\}} m_k \prod_{j=1}^{N} \frac{(Vb_j)^{m_j}}{m_j!\lambda^{dm_j}}\right] \Big/ Q_N(T,V), \qquad \sum_j jm_j = N \quad (2.14)$$

Note that since the b_j's are positive definite, the "statistical" weight factor $\prod_{j=1}^{N}(Vb_j)^{m_j}/m_j!\lambda^{dm_j}$ is well defined.

One can simplify Eq. (2.14) by defining an appropriate generating function. Starting with the generating function for a multinomial expansion,

$$\left(\sum_{k=1}^{\infty}\frac{x_k}{k!}t^k\right)^M = M!\sum_{N=M}^{\infty}\frac{t^N}{N!}\sum_{\{m_k\}}N!\prod_{k=1}^{N}\frac{1}{m_k!}\left(\frac{x_k}{k!}\right)^{m_k}, \qquad \sum km_k = N, \quad \sum m_k = M \quad (2.15)$$

where x_k is an arbitrary sequence, dividing both sides by $M!$, and then summing over M, we get

$$\exp\left(\sum_{k=1}^{\infty}\frac{x_k}{k!}t^k\right) = \sum_{N=0}^{\infty}\frac{t^N}{N!}\sum_{M=0}^{N}N!\sum_{\substack{\{m_k\}\\ \sum km_k=N,\ \sum m_k=M}}\prod_{k=1}^{N}\frac{1}{m_k!}\left(\frac{x_k}{k!}\right)^{m_k} \quad (2.16)$$

$$= \sum_{N=0}^{\infty}t^N\left\{\sum_{\substack{\{m_k\}\\ \sum_k km_k=N}}\prod_{k=1}^{N}\frac{1}{m_k!}\left(\frac{x_k}{k!}\right)^{m_k}\right\} \quad (2.17)$$

Note that, in deriving Eq. (2.16), we have interchanged sums. Now let $x_k = k!(Vb_k/\lambda^d)$. With this substitution Eqs. (2.15) and (2.17) provide equivalent generating functions one or the other of which is needed for

calculation of averages of thermodynamic quantities,

$$\exp\left(\lambda^{-d}V\sum_{k=1}^{\infty}b_k t^k\right)=\sum_{N=0}^{\infty}\frac{t^N}{N!}\left(\sum_{M=0}^{N}\sum_{M,N}\Gamma\right)=\sum_{N=0}^{\infty}t^N Z_N(T,V) \quad (2.18a)$$

where

$$\sum_{M,N}\Gamma = N!\sum_{\substack{\{m_k\}\\ \sum km_k=N,\ \sum m_k=M}}\prod_{k=1}^{N}\frac{1}{m_k!}\left(\frac{Vb_k}{\lambda^d}\right)^{m_k} \quad (2.18b)$$

By taking the partial derivative with respect to b_j on both sides of (2.17) one gets

$$\frac{V}{\lambda^d}b_j\sum_{N=0}^{\infty}\frac{t^{N+j}}{N!}N!\sum_{\substack{\{m_k\}\\ \sum km_k=N}}\prod_{k=1}^{N}\frac{\left[(V/\lambda^d)b_k\right]^{m_k}}{m_k!}$$

$$=\sum_{N=0}^{\infty}\frac{t^N}{N!}N!\sum_{\substack{\{m_k\}\\ \sum km_k=N}}\prod_{k=1}^{N}m_j\frac{\left(Vb_k/\lambda^d\right)^{m_k}}{m_k!} \quad (2.19)$$

The left-hand side of Eq. (2.19) is

$$\frac{Vb_j}{\lambda^d}\sum_{N=j}^{\infty}\frac{t^N}{(N-j)!}(N-j)!Z_{N-j} \quad (2.20)$$

Therefore,

$$\sum_{N=0}^{\infty}t^N\sum_{\substack{\{m_k\}\\ \sum km_k=N}}\prod_{k=1}^{N}m_j\frac{(Vb_k)^{m_k}}{m_k!\lambda^{dm_k}}=\frac{Vb_j}{\lambda^d}\sum_{N=j}^{\infty}t^N Z_{N-j} \quad (2.21)$$

Equation (2.21) permits writing $\bar{m}_k(T,V,N)$ in a form[6] that is simple to evaluate numerically:

$$\bar{m}_k(T,V,N)=\frac{Vb_k(T,V)}{\lambda^d}\frac{Z_{N-k}(T,V)}{Z_N(T,V)}, \qquad Z_N(T,V)=\frac{Q_N(T,V)}{N!} \quad (2.22)$$

[6] We thank the referee for suggesting the following simple derivation of Eq. (2.22). One rewrites (2.14) as

$$\bar{m}_k=\sum_{\substack{\{m_j\}\\ \sum_{j\neq k}jm_j+km_k=N}}\left[\prod_{j\neq k}\frac{(Vb_j)^{m_j}}{m_j!\lambda^{dm_j}}\frac{(Vb_k)^{m_k}}{(m_k-1)!\lambda^{dm_k}}\right]\Big/\,Q_N(T,V)$$

If one now lets the running variable $m_k\to m_{k+1}$, then the expression for $\bar{m}_k$ is precisely that given by Eq. (2.22).

The pressure of the system in the canonical ensemble is given by $P/k_BT = (\partial/\partial V)\ln Q_N(T,V)$. It may be shown that $V(\partial/\partial V)Q_N(T,V)$ can be put in the following form:

$$V\frac{\partial}{\partial V}Q_N(T,V) = \sum_{\substack{\{m_l\} \\ \sum lm_l = N}} \sum_{k=1}^{N} m_k \prod_{l=1}^{N} \frac{(Vb_l)^{m_l}}{m_l!\lambda^{dm_l}} + \sum_{\substack{\{m_l\} \\ \sum lm_l = N}} \sum_{k} m_k \frac{V}{b_k}\frac{\partial b_k}{\partial V} \prod_{l=1}^{N} \frac{(Vb_l)^{m_l}}{m_l!\lambda^{dm_l}} \tag{2.23}$$

Thus,

$$\frac{P}{k_BT} = \frac{1}{V}\sum_{k=1}^{N}\overline{m}_k(T,V,N) + \sum_{k=1}^{N}\overline{m_k(T,V,N)\frac{1}{b_k(T,V)}\frac{\partial b_k(T,V)}{\partial V}} \tag{2.24}$$

where the bar denotes an average over the canonical ensemble. If b_k is a function of the temperature only, then

$$\frac{PV}{k_BT} = \sum_{k=1}^{N}\overline{m}_k(T,V,N) = M(T,V,N) \tag{2.25}$$

Here, $M(T,V,N)$ is the total number of molecules in the system. Note that as $N/V \to 0$, $M(T,V,N) \to N$ and Eq. (2.25) gives the usual ideal gas equation of state. The effect of volume dependence is, thus, to renormalize $m_k : m_k \to m_k[1 + (V/b_k)(\partial b_k/\partial V)]$.

3. NUMERICAL RESULTS AND DISCUSSION

3.1. Volume-Independent Cluster Integrals

For every system of size N considered, the numerical calculation proceeds as follows:

First, for each temperature the $b_l(T)$ for $l \in [2,N]$ are computed with the use of Eq. (3.2).

Second, for each volume considered, the partition function $Q_l(T,V)$ is found with Eqs. (2.8) and (2.13), and the mean cluster size $\overline{m}_k(T,V,N)$ for $k \in [1,N]$ is computed with Eq. (2.22) from $Q_{N-k}(T,V)$ and the $b_k(T)$.

Finally, the canonical ensemble pressure is computed with Eq. (2.25).

A few technical aspects of the computer program, which enabled computation of the partition function of a system consisting of large numbers of particles, require discussion. The partition function at high

temperatures and large volumes behaves as

$$Q_N(T, V) \propto V^N \tag{3.1}$$

Thus, if $V = 40.8$ and $N = 90$, numerical evaluation of Eq. (3.1) in IBM 370/148 would give domain error. One way to avoid domain error is to exploit the scaling properties of Eq. (1.1). Such a procedure enables evaluation of $Q_N(T, V)$ for any $N \leqslant 100$ and for any density $V_0/V \in [0, 1]$. To handle values of $N \geqslant 120$ and numbers larger than 10^{75}, while preserving precision in computing, however, one must use floating point instructions with which the scaling is automatically done by the machine.

The procedure described here can be used to compute the equation of state and mean cluster size distributions for two- and three-dimensional ideal Bose gas systems among which the number of particles varies from $N = 128$ to $N = 1024$. The connected cluster integrals for an ideal d-dimensional Bose gas are known[3] to be given by

$$b_l = \frac{1}{l^{d/2+1}} \tag{3.2}$$

an expression that is valid as long as $(L/\lambda)^d \gg 1$.

Figure 1 shows a plot of $P\lambda^3/k_B T$ versus v/λ^3, where $v = V/N$. The smallest value of v/λ^3 that is accessible for numerical computation is restricted by the requirement $(L/\lambda)^3 \gg 1$. v/λ^3 is the "reduced" volume. We denote by $(v/\lambda^3)_B$ the reduced volume at which bimodality first appears in the mean cluster weight distribution. Figure 1 clearly shows that, although as expected in a finite system there is no sharp transition, there exist two regions having different compressibilities. As the number of particles in the system is increased, the pressure in the canonical ensemble

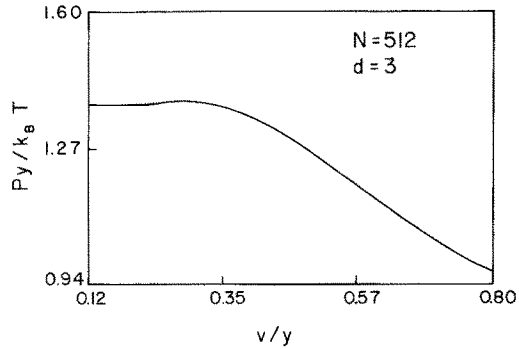

Fig. 1. Plot of Py/k_BT vs. v/y for $d = 3$, where d is the dimensionality of the system and $y = \lambda^3$.

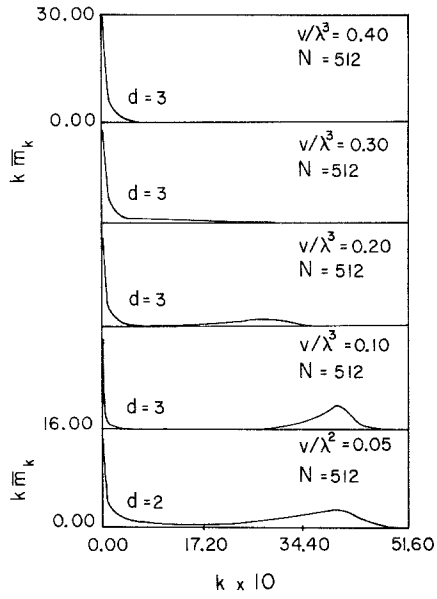

Fig. 2. Plot of $k\bar{m}_k$ as a function of k, for two- and three-dimensional ideal Bose gases.

seems to approach that in the grand canonical ensemble. (To be explicit, if the reduced volume is fixed at 0.1, for example, and $P\lambda^3/k_BT$ computed as a function of N, it is found that $(P\lambda^3/k_BT)|_{N=\infty} - (P\lambda^3/k_BT)|_{N=512} = 0.04$, and this is 0.02 when N is 1024.) From this it can be concluded that a system of 512 particles mimics thermodynamic behavior reasonably well.

The most important observation is that below a certain reduced volume the mean cluster weight distribution is bimodal, for a finite three-dimensional system approximated in this way (volume-independent cluster integrals). In Figure 2, $k\bar{m}_k$ has been plotted against k at four values of reduced volume, one above and three below the critical reduced volume,[3] $(v/\lambda^3)_c = 0.38$. The fraction of the weight of the system bound into clusters in a given size range is given by the area under each curve in that range. The second peak that exists below $(v/\lambda^3)_c$ grows continuously and uniformly as the reduced volume is decreased. Not only does the separation between the two peaks become more and more pronounced as v/λ^3 is decreased, but also the clusters represented in the second peak become more and more populated, eventually containing most of the particles of the system. Note that the values of $(v/\lambda^3)_B$ defined by the distributions $k\bar{m}_k$ are not the same as those for $k^2\bar{m}_k$. The numerical results show also that the rates of change of $(v/\lambda^3)_B$, as the system size is increased, are not

the same for $k\bar{m}_k$ and $k^2\bar{m}_k$. However, in both cases the rate of change of $(v/\lambda^3)_B$ decreases with increasing N; for both moments $(v/\lambda^3)_B$ approaches 0.38 in the thermodynamic limit.

The second peak in the mean cluster weight distribution represents macroscopic clusters, i.e., an accumulated phase. The first peak represents small clusters, i.e., the gas phase. That an accumulation is possible is realized on noting that, although there is no interparticle potential in an ideal Bose gas, there exist positive spatial correlations between bosons arising solely from the symmetry properties of the N-particle wave function. The strict analog of the classical Boltzmann factor is the function W_{BE}

$$W_{BE} = \sum_{\{\tilde{P}\}} \exp\left(- \frac{\pi}{\lambda^2} \sum_{k=1}^{N} |\mathbf{r}_k - \mathbf{r}_{\tilde{P}k}|^2 \right) \tag{3.3}$$

where $\tilde{P}$ is a permutation operator. Note that $W_{BE} \to 1$ when all the particles are far away from each other; $W_{BE} > 1$ in those regions of configuration space where some particles are near together. This corresponds to an *apparent attraction*[14] between the particles of an ideal Bose gas. This attraction *cannot* be represented by a potential which has the property of additivity. Since the potential is always attractive, there must be a correspondence between mathematical and physical clusters.

Analyzing the mean cluster weight distributions for systems consisting of 128, 256, and 512 particles, all at $v/\lambda^3 = 0.15$, one finds that, although the occupation numbers for the smallest clusters increase approximately linearly with N, those of medium size clusters do not: expressed as a fraction of N the latter appear to approach zero. The second peak accommodates an increasing population with increasing N in a different fashion from that seen in the first peak: the width of this second peak depicts a linear dependence on system size.

Figure 3 shows the dependence on v/λ^3 of the specific heat of a three-dimensional ideal gas of 256 bosons in this case for which volume-independent cluster integrals are used. The specific heat not only attains a rounded maximum, but displays the maximum slightly shifted to higher temperatures than in the case of the thermodynamic limit. C_v/Nk_B tends toward 3/2 as values of v/λ^3 are increased. On increasing the number of particles in the system one sees a sharper transition.

As expected, there is no sudden change in the slope of the graph of pressure vs. reduced density for a finite, two-dimensional ideal Bose gas (Fig. 4). However, close to $v/\lambda^2 \simeq 0.1$ the mean cluster weight distribution shows the gradual formation of a macroscopic cluster (Fig. 2). It has been rigorously established that fluctuations in the local order parameter are

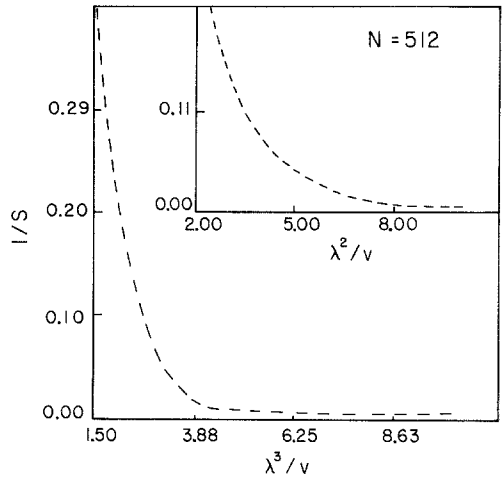

Fig. 3. The plot of inverse cluster size S^{-1} as a function of reduced volume for both two- and three-dimensional Bose gas.

large enough to destroy the formation of long-range order in a Bose fluid in systems of restricted dimensionality in the thermodynamic limit, provided that the density is bounded everywhere.[15,16] However, condensation cannot be excluded in a finite two-dimensional system.[17] In fact, a uniform, two-dimensional ideal Bose gas of finite area L^2 exhibits a condensation at

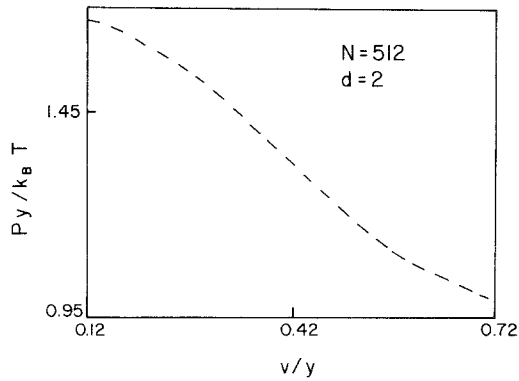

Fig. 4. Plot of Py/k_BT vs. v/y for $d = 2$, where d is the dimensionality of the system and $y = \lambda^2$.

a temperature approximately given by

$$T_0 \simeq \frac{2\pi h^2 \rho}{k_B m \ln N}, \qquad \rho = \frac{N}{L^2} \tag{3.4}$$

This corresponds to

$$\left(\frac{v}{\lambda^2}\right)_{T_0} \simeq \frac{1}{\ln N} \tag{3.5}$$

As the number of particles in the system is varied, the results indicate that, although the values of $(v/\lambda^2)_B$ for $k\bar{m}_k$ are approximately in the range predicted by Eq. (3.5), the correspondence with Eq. (3.5) is represented far more accurately by $k^2\bar{m}_k$. This is also the case in the finite three-dimensional Bose gas.

A useful property of the cluster distribution is the "weight average" mean cluster size S,[18] given by

$$S = \frac{\sum_{k=1}^{N} k^2 \bar{m}_k(T, V, N)}{N} \tag{3.6}$$

Figure 5 shows plots of S^{-1} vs. reduced volume for two- and three-dimensional Bose gases. The slopes in both graphs change most rapidly at the value of v/λ^d which signals the appearance of the second peak in $k\bar{m}_k$. Finally, it is noted that in the two-dimensional case the values of $(v/\lambda^2)_B$ for both moments approach zero as N gets large. This is consistent with Eq. (3.5), which predicts that $(v/\lambda^2)_{T_0}$ must be zero for a two-dimensional ideal

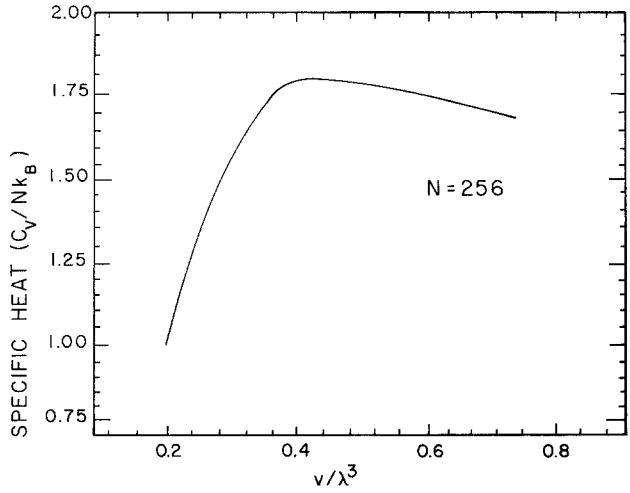

Fig. 5. Plot of specific heat (C_v/Nk_B) vs. v/λ^3 for three-dimensional ideal Bose gas. The number of particles in the system is $N = 256$.

Bose gas in the thermodynamic limit. Note that this behavior is different from that of the three-dimensional case, for which $(v/\lambda^3)_B$ approaches a nonzero value.

3.2. Bose Condensation and Polymer Gelation

The results of the last section indicate that similarities[5,9,10] exist between the Bose condensation of IBS and the sol→gel transition observed in the course of chemical polymerization of polyfunctional monomers.

Recent work of Donoghue and Gibbs[19] on the sol→gel transition in a finite polycondensing system has shown that the formation of a gel is signaled by the appearance of a second peak in the mean molecular weight distribution. Below a critical value of the extent of reaction, the mean number of polymers of size k is a monotonically decreasing function of size k, a size distribution corresponding to a pure sol phase. Beyond this critical degree of polymerization, however, there exists a second peak the maximum of which is located at a size k which is monotonically increasing function of the number of structural units N. This second peak, representing polymers of macroscopic size in macroscopic systems, is distinctive of the gel phase. It is interesting to compare the mean cluster size distributions of an ideal Bose gas obtained with volume-independent cluster integrals (in Section 3.1) to the mean cluster size distributions for the polymeric system computed by Donoghue and Gibbs.[19] Such an analysis has been recently carried out in detail.[5, 9, 10] Here we shall summarize the main results.

In both the sol→gel transition and the Bose–Einstein condensation, the mean cluster or polymer weight distribution is monotonic when either the extent of reaction (for polymers) or the density (for IBS) is less than a certain critical value. The large peak at small cluster size (maximum always at $k = 1$) represents sol molecules (mainly monomers and dimers) for polymer systems and excited particles in Bose systems. In both systems a second peak in the mean cluster weight distribution appears when a relevant variable (extent of reaction or density) exceeds a particular value. In IBS this second peak appears at a density which is close to the critical value determined by thermodynamic properties. Here the second peak in the bimodal cluster weight distribution represents the presence of a detectable fraction of particles in the ground state. In both systems, as the number of particles in the system is increased, the second peak moves to higher cluster sizes, whereas the first peak remains in place (maximum at $k = 1$) and increases in amplitude. Consequently, in macroscopic systems, the cluster sizes of the second peak are macroscopic. The qualitative features of the cluster size distributions are strikingly similar in the two cases.

In gelation theory, the quantities that play a role similar to that of the connected cluster integrals in a Bose gas are the $w_n(f)/n!$. $w_n(f)$ is defined as the number of distinguishable types of n-mers that can be made from n f-functional units when both functional units and monomers are distinguishable.[20] The quantity $w_n(f)$ is given by Stockmayer,[20] for the case when no ring formation is allowed, as

$$w_n(f) = f^n \frac{(fn - n)!}{(fn - 2n + 2)!} \tag{3.7}$$

The asymptotic form of $w_n(f)/n!$ is

$$\frac{w_n(f)}{n!} \propto n^{-5/2} \tag{3.8}$$

This is precisely the behavior of the volume-independent cluster integrals of an ideal three-dimensional Bose gas.

For the case of a classical gas in which an intermolecular potential is required for condensation, Born and Fuchs[21] have given an asymptotic form for the reducible cluster integrals $b_n(T)$'s,

$$b_n(T) \simeq n^{-5/2} \left(\sum_{k=1}^{n-1} k^2 \beta_k \zeta^k \right)^{-1} b_0^{-1} \tag{3.9}$$

where β_k is the kth star integral, b_0 is a constant, and ζ is a Lagrangian multiplier. Once again we note the appearance of the factor $n^{-5/2}$ in $b_n(T, V)$.

To emphasize the similarity between the sol→gel transition and BEC of an ideal Bose gas, we present, in Table I, the correspondence of analogous physical quantities.

One must bear in mind that neither of the two model systems participating in this analogy is an adequate model for any real system.

Table I. Analogies between Gelation and Bose–Einstein Condensation

Sol→gel transition	BEC of ideal Bose gas
Sol molecules	Particles in excited energy levels
Gel molecules	Condensed particles
Extent of reaction α	Reduced density λ^3/v
$\frac{w_n(f)}{n!}$ (no rings)	$b_n(T)$
Total number of macromolecules $M = \sum_{k=1}^{N} \bar{m}_k$	PV/Nk_BT
Functionality f	Not defined

Indeed, inclusion of volume dependence in the cluster integrals eliminates (see Section 3.3) the bimodality in the $k\bar{m}_k(T,V,N)$ distribution obtained for Bose particles and therefore destroys the analogy. Allowance for rings[10] in the structures allowed in gelation theory does, however, preserve the bimodality of the cluster size distribution given by that theory.

3.3. Volume-Dependent Cluster Integrals

In this section, a technique[10] is developed which enables calculation of the exact volume dependence of the connected cluster integrals $b_l(T,V)$ for IBS under Periodic boundary conditions, and the effect of this on the cluster size distribution is studied.

By definition, the average occupation number $\langle n_i \rangle$ for a Bose system is

$$\langle n_i \rangle = (e^{\alpha+\beta\epsilon_i} - 1)^{-1} \tag{3.10}$$

where $\alpha = -\mu/kT$, and μ is the chemical potential. The single particle energy ϵ_i can be obtained by solving a one-dimensional free particle Schrödinger equation subject to appropriate boundary conditions. We expand the average occupation number $\langle n_i \rangle$ in powers of $e^{\mu/kT}$:

$$N_{\text{av}} = \sum_i \langle n_i \rangle \tag{3.11}$$

$$= \sum_{j=1}^{\infty} e^{-j\alpha} \sum_i e^{-j\beta\epsilon_i} \tag{3.12}$$

For periodic boundary condition, the energy levels (for a three-dimensional system) $\epsilon_{n_1n_2n_3}$ can easily be shown to be

$$\epsilon_{n_1n_2n_3} = \frac{h^2}{2m}\left(\frac{n_1^2}{L_1^2} + \frac{n_2^2}{L_2^2} + \frac{n_3^3}{L_3^3}\right), \quad n_i = 0, \pm 1, \pm 2, \pm 3, \ldots, \qquad i = 1,2,3 \tag{3.13}$$

where L_1, L_2, and L_3 are the lengths of the sides of a rectangular box, and m is the mass of each Bose particle.

For convenience, we will consider the special case of a cubic system where $L_1 = L_2 = L_3 = L$. On rearranging Eq. (3.12) and on using (3.13), we get

$$N_{\text{av}} = \sum_{j=1}^{\infty} z^j \sum_{n_1,n_2,n_3=-\infty}^{\infty} \exp\left[-j\pi\left(n_1^2 + n_2^2 + n_3^2\right)\left(\frac{L}{\lambda}\right)^{-2}\right] \tag{3.14}$$

where z is the fugacity and λ is the thermal wavelength.

The connected cluster integrals $b_j(T, V)$ are defined by the relation

$$N_{\text{av}} = \frac{L^3}{\lambda^3} \sum j e^{-j\alpha} b_j(T, V) \tag{3.15}$$

On comparing Eq. (3.15) with Eq. (3.14), we can write down the volume-dependent cluster integral $b_j(T, V)$ as

$$jb_j = \left(\frac{\lambda}{L}\right)^3 \left[1 + 2\sum_{n=1}^{\infty} \exp\left(\frac{-j\pi n^2}{(L/\lambda)^2}\right)\right]^3 \tag{3.16}$$

For a finite system, one can use Eq. (3.16) to evaluate the cluster integrals. The infinite sum can be truncated after taking into account a sufficient number of terms, since the series is a rapidly convergent one. But the convergence is slow when the system size is increased. In order to obtain a series that is rapidly convergent for large system size we transform Eq. (3.16) by the use of Poisson summation formula. Let us start with the identity

$$\sum_{n=-\infty}^{\infty} F(n) = \sum_{q=-\infty}^{\infty} f(q) \tag{3.17}$$

where $f(q)$ is the Fourier transform of the function $F(n)$. Choosing $F(n)$ to be $e^{-j\omega n^2}$, we obtain the identity

$$\sum_{n=-\infty}^{\infty} e^{-j\omega n^2} = 2\sum_{q=-\infty}^{\infty} \int_0^{\infty} \cos(2\pi qn) e^{-j\omega n^2} dn \tag{3.18}$$

$$= \sum_{q=-\infty}^{\infty} \left(\frac{\pi}{j\omega}\right)^{1/2} e^{-\pi^2 q^2/j\omega} \tag{3.19}$$

where $\omega = \pi/(L/\lambda)^2$. Substituting Eq. (3.19) into Eq. (3.16) we get

$$jb_j = \frac{\lambda}{L}^3 \frac{\pi^{3/2}}{(j\omega)^{3/2}} \left[\sum_{q=-\infty}^{\infty} \exp\left(-\frac{\pi^2 q^2}{j\omega}\right)\right]^3 \tag{3.20}$$

Inserting the value of ω in Eq. (3.20) we get

$$jb_j(T, V) = \frac{1}{j^{3/2}} \left[\sum_{q=-\infty}^{\infty} \exp\left[-\frac{\pi q^2 (L/\lambda)^2}{j}\right]\right]^3 \tag{3.21}$$

Thus, the volume-dependent cluster integrals are

$$b_j(T, V) = \frac{1}{j^{5/2}} \left\{1 + 2\sum_{n=1}^{\infty} \exp\left[-\frac{n^2}{j}\pi (L/\lambda)^2\right]\right\}^3 \tag{3.22}$$

The above method can easily be generalized to any number of dimensions. In Appendix A, we have shown that Eq. (3.22) can also be derived

from the classical result of Walfisz[22] on the number of lattice points $N_d(x)$ in a hypersphere in d dimension of radius $x^{1/2}$.

The only errors that propagate in this method of calculation stem from the evaluation of $b_j(T, V)$. In this calculation, we have truncated the infinite sum over n in Eq. (3.22) by an upper bound $P = n_{\max}$, where $n_{\max} = 1024$. It is not necessary to assign such a large value to P, since the majority of the terms for n are essentially zero. Consider the elliptic function

$$\phi_3(0) = \left(\frac{2K}{\pi}\right)^{1/2} = 1 + 2\sum_{n=1}^{\infty} q^{n^2} \tag{3.23}$$

where $K(k)$ is

$$K(k) = \int_0^{\pi/2} \frac{d\phi}{(1 - k^2 \sin^2\phi)^{1/2}} \tag{3.24a}$$

and $q = e^{-\pi K'/K}$,

$$K' = K(k'), \qquad k' = (1 - k^2)^{1/2} \tag{3.24b}$$

From (3.22) and (3.23), one sees that

$$\left[j^{5/2} b_j(T, V)\right]^{1/3} = \phi_3(0) \tag{3.25}$$

provided that $K'/K = (L/\lambda)^2(1/j)$ and $q = \exp[-(\pi/j)(L/\lambda)^2]$ are chosen.

The errors involved in using Eq. (3.22) with all terms up to $n = P$ are now seen. For a typical value for q such as $q = 0.006585$, it is implied that $\pi K'/K = -5.0229609$, and from (3.25) it follows that $\phi_3(0) = 1.01316917$. By choosing $P = 20$ and calculating $[j^{5/2} b_j(T, V)]^{1/3}$ *from* Eq. (3.22) one gets 1.01317003. So even for small P the error is only in the sixth decimal place.

We here summarize briefly the main results of our calculations with the exact set of $b_k(T, V)$, with emphasis on the $k\bar{m}_k(T, V, N)$ distribution. An exhaustive study on the effect of system size on thermodynamic quantities, such as pressure, Helmoltz free energy, and specific heat under various boundary conditions, will be published[23] elsewhere.

The cluster weight distribution (Figs. 6–8) at various densities reveals the following features. (1) At large volumes, and for both $d = 2, 3$, the cluster weight distribution $k\bar{m}_k$ decreases monotonically with increasing k. (2) Below a critical reduced volume a "chair-shaped" cluster weight distribution appears, the absence of bimodality implying absence of diagonal long-range order (this point is discussed in Section 3.4). (3) The chair-shaped distributions for two- and three-dimensional IBS are characterized by ranges of k values for which $k\bar{m}_k = 1.00$. (4) The $k\bar{m}_k(T, V, N)$ distribution has different qualitative features in two and three dimensions: in three

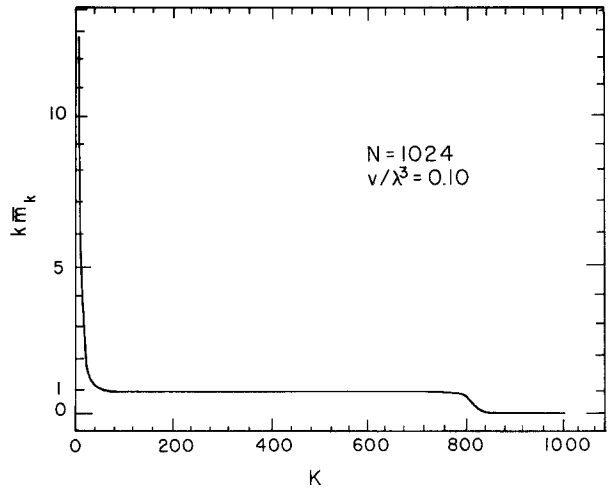

Fig. 6. The mean cluster weight distribution for three-dimensional periodic Bose gas as computed with volume-dependent cluster integrals, at $v/\lambda^3 = 0.10$. Abscissa k is the cluster size and ordinate $k\bar{m}_k$ gives the occupation number $\bar{m}_k$ of cluster size k multiplied by k.

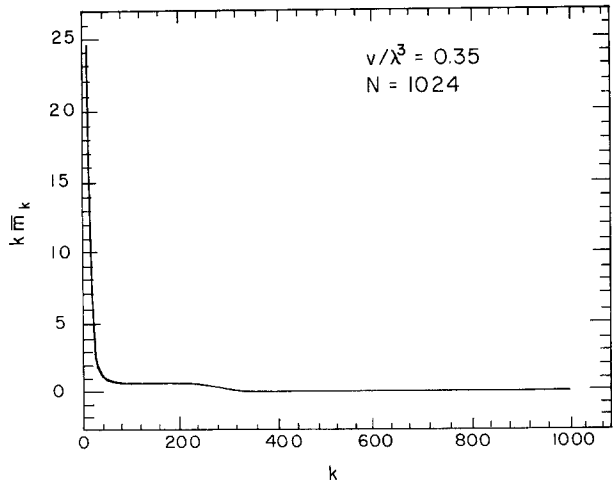

Fig. 7. The mean cluster weight distribution for three-dimensional periodic Bose gas as computed with volume-dependent cluster integrals, at $v/\lambda^3 = 0.35$. Abscissa k is the cluster size and ordinate $k\bar{m}_k$ gives the occupation number $\bar{m}_k$ of cluster size k multiplied by k.

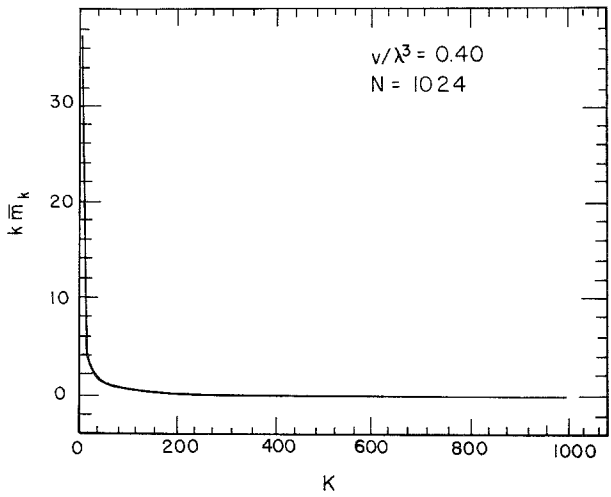

Fig. 8. The mean cluster weight distribution for three-dimensional periodic Bose gas as computed with volume-dependent cluster integrals, at $v/\lambda^3 = 0.40$. Abscissa k is the cluster size and ordinate $k\bar{m}_k$ gives the occupation number $\bar{m}_k$ of cluster size k multiplied by k.

dimensions for all reduced volume v/λ^3 less than 0.30, increasing N increases the range of k values for which $k\bar{m}_k$ is precisely one, the same effect being achieved by fixing N and choosing progressively smaller values of v/λ^3; in two dimensions for a given $v/\lambda^2 < (v/\lambda^2)_B \approx 0.12$, increasing N *decreases* this range of k values, this result being consistent with the theorem of Mermin and Hohenberg,[15,16] which states the impossibility of a Bose condensation in an infinite two-dimensional IBS system. (5) In three dimensions the value of $v/\lambda^3 (\approx 0.3)$ at which the chair-shaped distribution first appears *does* not coincide with the value of v/λ^3 at which the *maximum* of the specific heat data occurs[23]; in two dimensions there is *no* specific heat maximum; thus, the location of a maximum in specific heat as a function of T is not a general crtierion of BEC in finite IBS.

The results for the size distribution of clusters can be understood in terms of the absence of diagonal long-range order (DLRO) of IBS in the canonical ensemble. We discuss this in some detail in Appendix B.

3.4. Summary

The expansion of the canonical partition function, involving the cluster integrals, has been shown to be related to a set of polynomials, the so-called

Bell polynomials[12]. This observation has permitted derivation of a recursion relation[12] for the partition function, which, in turn, has rendered numerical evaluation of thermodynamic quantities tractable.

With volume-independent cluster integrals, the key observation has been that, below a certain reduced volume, the mean cluster weight distribution becomes bimodal for finite two- and three-dimensional ideal Bose systems. The first peak represents small clusters, corresponding to the gaseous phase. It has also been seen that, even though the occupation numbers for the smallest clusters increase approximately linearly with N, the fractional occupations of medium-size clusters approach zero. The second peak at large sizes has been identified as representing the occurrence of macroscopic clusters in the mean cluster weight distribution, i.e., an accumulated phase. In accommodates increasing mass with increasing N by an increase in cluster sizes rather than in occupations of each size. This "horizontal scaling" of the condensate peak, as contrasted with the vertical scaling of the gas peak, clearly demonstrates the macroscopic nature of the "liquid" clusters in a macroscopic system.

In many respects, the behavior of this bimodal distribution is remarkably similar to that obtained by Donoghue and Gibbs in a recent study of gelation in a finite nonlinear polymerizing system. For nonlinear polymers, a gel peak appeared naturally in the mean molecular weight distribution as the degree of polymerization was increased. The similarity between Bose condensation and gelation has been discussed in detail in Section 3.2. The analog was valid strictly for BEC of an ideal three-dimensional Bose gas in the grand canonical ensemble.

The mean cluster weight has been seen to acquire a chair-shaped distribution instead of a bimodal distribution when the exact volume dependence of the cluster integrals is taken into account. This implies the absence of diagonal long-range order of IBS in the canonical ensemble.[24,25]

A remarkable property that has been seen in the $k\bar{m}_k(T, V, N)$ distributions for both two- and three-dimensional IBS is that ranges of k values exist for which $k\bar{m}_k = 1.0$. In the two-dimensional case, for a given $v/\lambda^2 < (v/\lambda^2)_B$, increasing N decreases the range of k values for which $k\bar{m}_k \simeq 1.0$. This result is consistent with the theorem of Mermin and Hohenberg, which states the impossibility of Bose condensation in infinite two-dimensional IBS (provided the density is bounded everywhere).

The form the Kac density[24,25] for ideal Bose systems rigorously implies that, although thermodynamic properties agree in the canonical and the grand canonical ensemble, fluctuations in the ground state do not agree. The Ursell functions have a cluster property, provided the particles are widely separated. A consequence of this result is that IBS do not exhibit DLRO in the canonical ensemble.

We propose that the appearance of a second peak well separated from the first in the average cluster weight distribution can be viewed as a physical criterion for the existence of diagonal long-range order in quantum systems displaying phase transitions. For the case of IBS, the value of temperature at which the mean cluster weight acquires a chair-shaped distribution is a more fundamental determinant of the BEC in finite systems (in the canonical ensemble) than the location of a specific heat maximum as a function of T. If the IBS is subjected to an external field, the chair-shaped distribution for the average cluster weight becomes a bimodal distribution.

APPENDIX A

In this Appendix we show that the volume dependence of the connected cluster integrals of a three-dimensional IBS can be calculated from the classical result of Walfisz[22] on the number of lattice points $N_d(x)$ in a hypersphere in d dimensions of radius $x^{1/2}$. This number of lattice points is given by

$$N_d(x) = \frac{\pi^{d/2}}{\Gamma(1+d/2)} + x^{d/4} \sum_{\substack{n_1,n_2,n_3=-\infty \\ n^2=n_1^2+n_2^2+n_3^2}} n^{-d/4} J_{d/2}\left[2\pi(xn)^{1/2}\right] \quad \text{(A1)}$$

with $J_{d/2}$ denoting the Bessel function of order $d/2$. Formal differentiation of (3.15) leading to the lattice-point density $\rho_d(x)$ has been rigorously justified by Oppenheim,[26] who has shown that

$$\rho_1(x) = x^{-1/2} \sum_{n_1=-\infty}^{\infty} \cos\left(2\pi(nx)^{1/2}\right) \quad \text{(A2)}$$

$$\rho_2(x) = \pi \sum_{n_1,n_2=-\infty}^{+\infty} J_0\left(2\pi(nx)^{1/2}\right) \quad \text{(A3)}$$

$$\rho_3(x) = 2\pi x^{1/2} \sum_{n_1,n_2,n_3=-\infty}^{\infty} \frac{\sin\left(2\pi(nx)^{1/2}\right)}{2\pi(nx)^{1/2}} \quad \text{(A4)}$$

Boundary conditions lead to the relation

$$\rho(\lambda) = (1/8)\{\rho_3(\lambda) + 3\theta\rho_2(\lambda) + \theta\rho(\lambda)\} \quad \text{(A5)}$$

where $\lambda = \pi x/L = k^2$. Combining Eqs. (A2), (A3), (A4), and (A5), one gets

$$\rho(k) = \frac{L^3k^2}{2\pi^2} \sum_{n_1,n_2,n_3=-\infty}^{\infty} \frac{\sin(2kn^{1/2})}{2kLn^{1/2}} + \theta\frac{3L^2k}{4\pi} \sum_{n_1,n_2=-\infty}^{\infty} J_0(2kLn^{1/2}) + \frac{3L}{4\pi} \sum_{n_1=-\infty}^{\infty} \cos(2kLn^{1/2}) + \theta\frac{1}{8}\delta(k) \quad \text{(A6)}$$

where $\theta = 0, -1, +1$ for periodic, Dirichlet, and Neumann boundary

conditions, respectively. In the case of the periodic boundary conditions, the average number of bosons N in a finite three-dimensional cubical box is now seen to be

$$N_{\text{av}} = \frac{L^3}{\lambda^3} \sum_{j=1}^{\infty} e^{-j\alpha} \left\{ \frac{1}{j^{3/2}} \sum_{n=-\infty}^{\infty} \exp\left[-\frac{n^2\pi}{j} (L/\lambda)^2 \right] \right\}^3 \tag{A7}$$

Hence, the connected cluster integrals got from Eq. (A7) agree with that given by Eq. (3.22).

APPENDIX B

The ideal Bose gas exhibits diagonal long-range order in the grand canonical ensemble.[27] It was demonstrated in Section 3.3 that use of the exact volume dependence of $b_j(T, V)$ leads to an absence of bimodality in the cluster size distribution in the canonical ensemble. To understand this result we investigate, in this appendix, the existence or nonexistence of diagonal long-range order of IBS in the canonical ensemble.

In the grand canonical ensemble, let the generating function of any canonical function X be denoted by

$$X_{\text{gr}}(\alpha, T, \Lambda) \equiv \sum_{N=0}^{\infty} e^{-\alpha N} X \frac{Z(N, \Lambda, T)}{Z_{\text{gr}}(\alpha, \Lambda, T)} \tag{B1}$$

where Λ denotes the bounded region with volume V. Let the corresponding canonical ensemble thermodynamic limit quantities be denoted by

$$X(\rho, T) \equiv \lim_{V \to \infty} X(N, \Lambda, T), \qquad \rho = \frac{N}{V} \tag{B2}$$

Further, let

$$X_{\text{g}}(\alpha, T) \equiv \lim_{V \to \infty} X_{\text{g}}(\alpha, \Lambda, T)$$

where α is determined by the sum rule

$$\rho = \frac{N_{\text{gr}}}{V} = \sum_{N=0}^{\infty} N e^{-\alpha N} \frac{Z(N, \Lambda, T)}{Z_{\text{gr}}(\alpha, \Lambda, T)} \tag{B3}$$

Clearly, $X(\rho, T)$ and $X_{\text{g}}(\rho, T)$ are related to each other by Kac density[24,25] $K(x, \rho, T)$

$$X_{\text{g}}(\rho, T) = \int_0^{\infty} K(x, \rho, T) X(x, T)\, dx, \qquad x = \frac{N}{V} \tag{B4}$$

where

$$K(x, \rho, T) \equiv \lim_{V \to \infty} V e^{-\alpha N} \frac{Z(N, \Lambda, T)}{Z_{\text{gr}}(\alpha, \Lambda, T)}$$

First, it will be shown that for an IBG in which density is such that $\rho < \rho_c$, the canonical and the grand canonical states are the same. Above the critical density, the grand canonical states are the Laplace transform of the canonical states.[25, 28]

Since the characteristic function is defined as

$$\left\langle e^{i\tau \frac{N}{V}} \right\rangle \equiv \frac{Z_{\mathrm{gr}}(\alpha - i\tau/V, \Lambda, T)}{Z_{\mathrm{gr}}(\alpha, \Lambda, T)} \tag{B5}$$

we have

$$\lim_{V\to\infty} \left\langle e^{i\tau \frac{N}{V}} \right\rangle = \int_0^\infty K(x,\rho) e^{i\tau x}\, dx \tag{B6}$$

But,

$$\ln\left\langle e^{i\tau \frac{N}{V}} \right\rangle \sim \frac{i\tau g_{3/2}(\alpha)}{\lambda^3} = i\tau\rho, \qquad \text{for } \rho < \rho_c \tag{B7}$$

where $g_\sigma(\alpha)$ is the familiar Bose function.[3] Thus from Eqs. (B4) and (B7) we see that $K(x,\rho) = \delta(x-p)$ for $\rho < \rho_c$. If $\rho > \rho_c$, one must keep the '$k = 0$' term in Z_{gr} and then let $\alpha \to 0$ *as* $L \to \infty$

$$\ln\left\langle \exp i\tau \frac{N}{V} \right\rangle = \left(\frac{L}{\lambda}\right)^3 \left[\frac{i\tau}{L^3}\, g_{3/2}(\alpha)\right] - \ln \frac{\alpha - i\tau/V}{\alpha} \tag{B8}$$

In Eq. (B8) one can put $\alpha = 0$ in $g_{3/2}$ but for consistency $\alpha^{-1} = L^3(\rho - \rho_c)$ must be used in the logarithmic terms. Simple algebra then yields

$$\left\langle e^{i\tau \frac{N}{V}} \right\rangle \sim e^{i\tau\rho_c}\left[1 - i(\rho - \rho_c)\tau\right]^{-1} \tag{B9}$$

The right-hand side of Eq. (B9) can be rewritten as

$$\frac{1}{\rho - \rho_c} \int^\infty dx \exp\left(-\frac{x - \rho_c}{\rho - \rho_c}\right) \exp(-i\tau x) \tag{B10}$$

All of the steps discussed above have been rigorously derived by Kac[24,25] (unpublished), Cannon,[28] Lewis and Pule.[29]

The Kac density for the IBG can be summaried as

$$K(x,\rho) = \begin{cases} \delta(x-\rho), & \rho < \rho_c \\ \left[\begin{array}{l} 0, \; x < \rho_c, \\ (\rho - \rho_c)^{-1} \exp\left(-\dfrac{x - \rho_c}{\rho - \rho_c}\right), \; x > \rho_c, \end{array}\right] & \rho > \rho_c \end{cases} \tag{B11}$$

For $\rho > \rho_c$ and with $K(x,\rho)$ given by (B11), Eq. (B4) relating $X_{\mathrm{g}}(\alpha,\rho,T)$ to $X(\rho,T)$ is basically a Laplace transform. The inverse Laplace transform

thus yields

$$X(\rho, T) = \frac{1}{2\pi i} \oint \frac{dt}{t} e^{(\rho - \rho_c)t} X_g\left(\rho_c + \frac{1}{t}, T\right) \tag{B12}$$

where the contour of integration goes around the origin in the positive sense. Using the Kac density, the bulk limit of grand canonical density matrices, and the inverse formula (B12) enables us to write down the s-particle density matrix in the canonical ensemble

$$\rho_s(\mathbf{r}'^s, \mathbf{r}''^s, \alpha, T) = \begin{cases} \displaystyle\sum_{P\{r'^s\}} \prod_{i=1}^{s} A(|\mathbf{r}'_i - \mathbf{r}''_i|, \alpha, T), & \rho < \rho_c \\ \displaystyle\sum_{P\{r'^s\}} \frac{1}{2\pi i} \oint \frac{dt}{t} \sum_{m=0}^{\infty} \frac{\exp\{m \ln[t(\rho - \rho_c)]\}}{m!} & \\ \quad \times \displaystyle\prod_{i=1}^{\infty} \left[(A|\mathbf{r}'_i - \mathbf{r}''_i|, 0, T) + \frac{1}{t} \right], & \rho > \rho_c \end{cases} \tag{B13}$$

where

$$A(|\mathbf{r}'_i - \mathbf{r}''_i|, \alpha, T) \equiv \frac{1}{\lambda^3} \sum_{j=1}^{\infty} \frac{\exp(-\alpha j)}{j^{3/2}} \exp\left(- \frac{\pi}{j\lambda^2} |\mathbf{r}'_i - \mathbf{r}''_i|^2 \right) \tag{B14}$$

As $|\mathbf{r}'_1 - \mathbf{r}''_1| \to \infty$, $A \to 0$. Hence, the single-particle density matrix becomes

$$\rho_1(\mathbf{r}'_1, \mathbf{r}''_1, \rho, T) \to \begin{cases} 0, & \rho < \rho_c \\ \rho - \rho_c, & \rho > \rho_c \end{cases} \tag{B15}$$

The two-particle density matrix is given in the off-diagonal limit by

$$\rho_2 \to \begin{cases} 0, & \rho < \rho_c \\ (\rho - \rho_c)^2, & \rho > \rho_c \end{cases} \tag{B16}$$

The diagonal element of ρ_2 is the two-particle distribution function

$$n_2(\mathbf{r}_1, \mathbf{r}_2, \rho, T) = \begin{cases} \rho^2 + [A(|\mathbf{r}_1 - \mathbf{r}_2|, \alpha, T)]^2, & \rho < \rho_c \\ \rho^2 + 2(\rho - \rho_c) A(|\mathbf{r}_1 - \mathbf{r}_2|, 0, T) & \\ \quad + [A(|\mathbf{r}_1 - \mathbf{r}_2|, 0, T)]^2 & \rho > \rho_c \end{cases} \tag{B17}$$

As $|\mathbf{r}_1 - \mathbf{r}_2| \to \infty$, $n_2 \to \rho^2 = n_1(r_1) \times n_1(r_2)$. The two-particle distribution function has the product property. Thus, the Ursell functions defined by

$$\begin{aligned} n_1(\mathbf{r}_1) &= U_1(\mathbf{r}_1) \\ n_2(\mathbf{r}_1, \mathbf{r}_2) &= U_2(\mathbf{r}_1, \mathbf{r}_2) + U_1(\mathbf{r}_1) U_2(\mathbf{r}_2) \end{aligned} \tag{B18}$$

must have the *cluster* property, i.e., $U_2(\mathbf{r}_1, \mathbf{r}_2) \to 0$ in the limit $|\mathbf{r}_1 - \mathbf{r}_2| \to \infty$. Physically, this implies that there is *no* diagonal long-range order (DLRO) in the canonical ensemble. In other words, there is no phase separation[30] in spite of the fact that the form of Kac density rigorously implies the equivalence of bulk thermodynamic properties in the two different ensembles.

The canonical ensemble s-particle density matrix in the off-diagonal limit is

$$\rho_s = \begin{cases} 0, & \rho < \rho_c \\ (\rho - \rho_c)^s, & \rho > \rho_c \end{cases} \tag{B19}$$

In the off-diagonal limit, $|\mathbf{r}' - \mathbf{r}''| \to \infty$, the s-particle density matrix for the ideal Bose gas in the grand canonical ensemble can be shown to be

$$\rho_s^{\mathrm{gr}}(\mathbf{r}'^s, \mathbf{r}'^s, \rho, T) = \begin{cases} 0, & \rho < \rho_c \\ s!(\rho - \rho_c)^s, & \rho > \rho_c \end{cases} \tag{B20}$$

The above results imply that in the grand canonical ensemble, the s-particle distribution function *does not* have the product property for $\rho > \rho_c$. In fact, in the limit where all the coordinates are widely separate the corresponding Ursell functions are given by

$$U_s^{\mathrm{gr}} = \begin{cases} 0, & \rho < \rho_c \\ (s-1)!(\rho - \rho_c)^2, & \rho > \rho_c \end{cases} \tag{B21}$$

Therefore, the grand canonical system *exhibits diagonal long-range order* (DLRO) and *there is* a phase separation.

To summarize, the ideal Bose systems do not exhibit diagonal long-range order in the canonical ensemble, but do so in the grand canonical. In other words, no phase separation exists in the former as in the latter. However, the form the Kac density rigorously implies the equivalence of bulk thermodynamic properties in the canonical and the grand canonical ensembles. We can relate this situation to the contrasting numerical results of Section 3.1 and 3.3 for the canonical ensemble. On one hand, the volume-independent cluster integrals of IBS lead to a bimodality in the cluster weight distribution, thereby reflecting the existence of DLRO, whereas the exact volume-dependent $b_l(T, V)$ do not lead to a phase separation. On the other hand, as N increases, thermodynamic quantities such as pressure and specific heat calculated with both the volume-dependent and the volume-independent cluster integrals tend to agree reasonably well over the range of densities (see Section 3.1) considered in this paper.

REFERENCES

1. M. F. M. Osborne, *Phys. Rev.* **76**:396 (1949); J. M. Ziman, *Philos. Mag.* **44**:548 (1953); D. L. Mills, *Phys. Rev.* **134**:A306 (1964); B. M. Khorana and Douglass, *Phys. Rev.* **138**:A35 (1965); D. A. Krueger, *Phys. Rev. Lett.* **19**:563 (1967); D. F. Goble and L. E. H. Trainor, *Can. J. Phys.* **44**:27 (1966); D. F. Goble and L. E. H. Trainor, *Can. J. Phys.* **46**:1867 (1968).
2. R. K. Pathria, *Phys. Rev.* A **5**:1451 (1972); S. Greenspoon and R. K. Pathria, *Phys. Rev.* A **8**:2657 (1973); S. Greenspoon and R. K. Pathria, *Phys. Rev.* A **9**:2103 (1974); M. N. Barber and M. E. Fisher, *Phys. Rev.* A **8**:1124 (1972); A. N. Chaba and R. K. Pathria, *Phys. Rev.* A **11**:1080 (1975).
3. R. K. Pathria, *Statistical Mechanics* (Pergamon Press, New York, 1978).
4. E. T. Bell, *Ann. Math.* **35**:258 (1938).
5. U. Mohanty, Ph.D. thesis, Brown University (1980).
6. U. Mohanty, A. Yang, and J. H. Gibbs, (in preparation).
7. J. H. Gibbs, B. Bagchi, and U. Mohanty, *Phys. Rev. B* **24**:2893 (1981).
8. J. A. Barker, P. J. Leonard, and A. Pompe, *J. Chem. Phys.* **44**:4206 (1966).
9. F. E. Harris, *J. Chem. Phys.* **23**:1518 (1955).
10. B. Bagchi, Ph.D. thesis, Brown University (1980).
11. G. C. Rota, *Finite Operator Calculus* (Academic Press, New York, 1975); S. Roman and G. C. Rota, *Adv. Math.* **27**:95 (1978).
12. U. Mohanty, *J. Math. Phys.* (July, 1982).
13. G. E. Uhlenbeck and G. W. Ford, in *Lectures in Statistics Mechanics* (American Mathematical Society, Providence, Rhode Island, 1963).
14. G. E. Uhlenbeck and L. Gropper, *Phys. Rev.* **41**:79 (1932).
15. P. C. Hohenberg, *Phys. Rev.* **158**:383 (1967).
16. J. J. Rehr and N. D. Mermin, *Phys. Rev. B* **1**:3160 (1970).
17. Y. Imry, *Physica* **55**:344 (1971).
18. A. Coniglio, V. DeAngelis, and A. Forlari, *J. Phys. A: Math. Gen.* **10**:1123 (1977); see also D. Stauffer, *Phys. Rep.* **43**:1 (1979).
19. E. Donoghue and J. H. Gibbs, *J. Chem. Phys.* **70**:2346 (1979).
20. W. H. Stockmayer, *J. Chem. Phys.* **11**:45 (1943).
21. M. Born and Fuchs, *Proc. R. Soc. London Ser. A* **166**:391 (1938).
22. A. Walfisz, *Z. Math.* **19**:300 (1924).
23. B. Bagchi and U. Mohanty (in preparation).
24. M. Kac (unpublished work); see E. B. Davis, *Commun. Math. Phys.* **30**:229 (1973).
25. R. Ziff, G. Uhlenbeck, and M. Kac, *Phys. Rep.* **32**:169 (1977).
26. A. Oppenheim, *Proc. London Math. Soc.* **26**:295 (1926); H. P. Boltes and B. Steinle, *J. Math. Phys.* **18**:1275 (1977).
27. C. N. Yang, *Rev. Mod. Phys.* **34**:694 (1962); O. Penrose and L. Onsager, *Phys. Rev.* **104**:576 (1956).
28. J. T. Cannon, *Commun. Math. Phys.* **29**:89 (1973).
29. J. T. Lewis and J. V. Pulé, *Commun. Math. Phys.* **36**:1 (1974).
30. G. E. Uhlenbeck, P. C. Hemmer, and M. Kac, *J. Math. Phys.* **4**:229 (1963).